

SYNTHESIS ZTO NANOPARTICLES AND STUDY OF THEIR PHOTOCATALYTIC PROPERTIES

N. BULUT^a, O. BAYTAR^b, Ö. ŞAHİN^b, S. HOROZ^{c,*}

^a*Siirt University, Institute of Science and Technology, Siirt, 56100, Turkey*

^b*Siirt University, Faculty of Engineering, Department of Chemical Engineering, Siirt, 56100, Turkey*

^c*Siirt University, Faculty of Engineering, Department of Electrical & Electronics Engineering, Siirt, 56100, Turkey*

Nanosized zinc tin oxide (ZTO, Zn_2SnO_4) photocatalysts were prepared with a hydrothermal technique and their structural and optical properties were characterized by performing powder x-ray diffraction (XRD), ultraviolet-visible (UV-Vis) and photoluminescence (PL) spectroscopies, respectively. The XRD results indicated that the ZTO nanoparticles have a face-centered cubic spinel structure and the average crystallite size was calculated as 18.75 nm by using the Debye-Scherrer equation. The band gap of ZTO nanoparticles was determined as 3.87 eV which is higher than that of bulk ZTO (3.6 eV). The effect of some parameters (amount of dye, amount of catalyst and temperature) were studied on the photocatalytic activity of ZTO nanoparticles. The obtained all results revealed that ZTO nanoparticles can be used as promising photocatalysts for degradation methyl-blue (MB) (dye). Moreover, it was determined that photocatalytic degradation kinetics of dye at all temperatures are better matched to the first order kinetic model.

(Received January 8, 2019; Accepted April 12, 2019)

Keywords: Characterization, Metal oxide, Nanoparticles, Photocatalytic, Synthesis

1. Introduction

Photocatalytic activity is induced by exposure of semiconductor material to radiation. The energy of this radiation must be equal to or greater than the band gap energy of that semiconductor material [1-3]. An electron in the valence band of semiconductor material is excited by exposure to radiation and passes into the empty conduction band. Thus, that electron creates an electron vacancy in the valence band. The free electron in the conduction band and the electron vacancy in the valence band cause the formation of active species which result in photocatalytic degradation [4, 5]. Both charge carriers move to the surface of the photocatalyst and react with the molecules on the semiconductor surface [6]. The free electron in the conduction band converts the oxygen into superoxide and hydroperoxide radicals by the reduction reaction while the electron vacancy in the valence band converts the water into hydroxyl radicals by the oxidation reaction. The resulting reactive species (superoxide, hydroperoxide and hydroxyl) lead degradation of the components that come in contact with the semiconductor material [7-9].

Metal oxide semiconductors have an important place among semiconductor materials. Among the metal oxide semiconductor materials, zinc tin oxide (ZTO, Zn_2SnO_4), which has positive properties such as high chemical stability, low-cost production and high reactive index, has been the focus of researchers in recent years. ZTO with the band gap energy of 3.6 eV has been used as a promising material in various applications such as the gas sensor, solar cells and photocatalysis [10-12].

The techniques used for the synthesis of ZTO in the last decade can be listed as sol-gel [13] chemical precipitation [14], hydrothermal [15] and calcination at high temperature [16]. Among these methods, the hydrothermal technique is a very important method since it allows the

* Corresponding author: sabithoroz@siirt.edu.tr

synthesis of particles having excellent crystal quality because the reaction temperature is below 200 °C. This synthesis method provides the formation of high-quality nanoparticles without impurities in the solution. Moreover, the hydrothermal technique allows for the production of many nanoparticles. The only disadvantage of this method is the need for an expensive autoclave system [17].

In the present study, the photocatalytic activity of ZTO nanoparticles (catalyst) was investigated. Some parameters (amount of dye, amount of catalyst and temperature) were studied on the photocatalytic activity of the catalyst. Moreover, the structural and optical properties of catalyst synthesized by hydrothermal technique were investigated.

2. Experimental study

Chemicals

The chemical reagents have been analytical grade and been used as obtained without further purification. The hydrothermal synthesis method was used to prepare ZTO nanoparticles. Zinc acetate dihydrate ($\text{Zn}(\text{CH}_3\text{COO})_2 \cdot 2\text{H}_2\text{O}$) and tin chloride pentahydrate ($\text{SnCl}_4 \cdot 5\text{H}_2\text{O}$) as starting materials, NaOH as a mineralizing agent, deionized water (DIW) and ethanol as solvents, have been used.

Synthesis of Catalyst

0.0015 moles $\text{SnCl}_4 \cdot 5\text{H}_2\text{O}$ and 0.003 moles $\text{Zn}(\text{CH}_3\text{COO})_2 \cdot 2\text{H}_2\text{O}$ were added in 20 mL of ethanol under magnetic stirring. 0.45 M NaOH was dissolved in 20 mL of DIW. Then, the aqueous solution of NaOH was dropped into the above solution. The solution was stirred for half an hour. The obtained mixture was transferred to a 100mL Teflon-lined autoclave and then maintained at 120°C for 24 h. As a final step, the autoclave was cooled down to room temperature and the sample was removed from the solvent by filtration paper. The obtained white sample was washed several times with absolute ethanol and distilled water and finally dried at 80°C in air for 5 h to get the final products.

Characterizations

X-ray diffraction (XRD) in a Rigaku x-ray diffractometer with $\text{Cu K}\alpha$ ($\lambda = 1,54 \text{ \AA}$) radiation was used to characterize the structural properties of the catalyst. Optical characterization was carried out by ultraviolet-visible (UV-Vis) and photoluminescence (PL) spectroscopies on a Perkin-Elmer Lambda 2 and a Perkin-Elmer LS 50B, respectively. For measurement of the photocatalytic activity of catalyst; 20 mg methyl-blue (MB) (dye) was dissolved in 1L DIW. Then, 30 mg catalyst was suspended in 100 mL an aqueous solution of the dye. The solution was placed below the UV-lamb. The suspensions were stirred for 30min before UV-light irradiation to provide absorption-desorption equilibrium. The 3mL reaction catalyst solution was taken out from the system at a certain time interval and then centrifuged to remove the solid catalyst. After that, the obtained dye solution was analyzed on a UV-Vis spectrophotometer in the wavelength range of 200–700 nm.

3. Results and discussions

Structural properties

XRD measurement

XRD measurement was performed to analyze the phase structure and purity of catalyst synthesized by hydrothermal synthesis method. The XRD patterns of catalyst are indicated in Fig. 1.

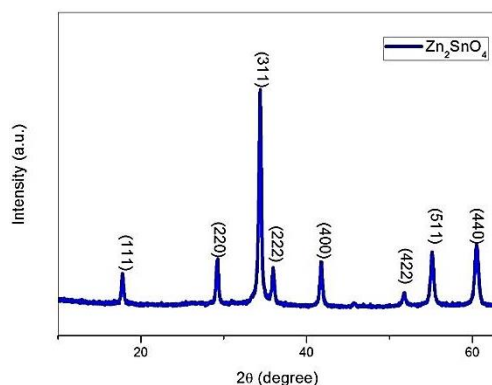


Fig. 1. The XRD patterns of catalyst prepared via hydrothermal synthesis method.

The obtained XRD data is consistent with the standard JCPDS powder diffraction file no: 24-1470. It can be seen that the catalyst has the formation of face-centered cubic spinel structure with the lattice constant $a = 8.66 \text{ \AA}$. Unwanted peaks from other crystal structure are not detected in the XRD data of ZTO nanoparticles. This result is an indication that the catalyst was synthesized by hydrothermal synthesis method. Sepelak et al.[18] mentioned that the crystallinity and size of sample synthesized using a hydrothermal process can be affected by the alkaline concentration. Our XRD result shows that the synthesized catalyst is close to the expected stoichiometric ratio.

The Scherrer relation [19] was used to calculate the mean crystallite size of catalyst.

$$d = 0.9 \lambda / (\beta \cos \theta) \quad (1)$$

where d is the mean size of the thin film, λ is the wavelength of x-ray, β is the broadening measured as the full width at half maximum (FWHM) in radians and θ is Bragg's diffraction angle. The calculated mean crystallite size of the catalyst is 18.75 nm . This result suggests that the catalyst with narrow size distribution and high purity can be synthesized via hydrothermal synthesis technique.

Optical properties

Optical absorption measurement

The optical absorption measurement was carried out to analyze the optical properties and energy structures of catalyst synthesized via hydrothermal synthesis technique. Fig. 2a indicates the recorded UV-vis absorption spectrum for the catalyst.

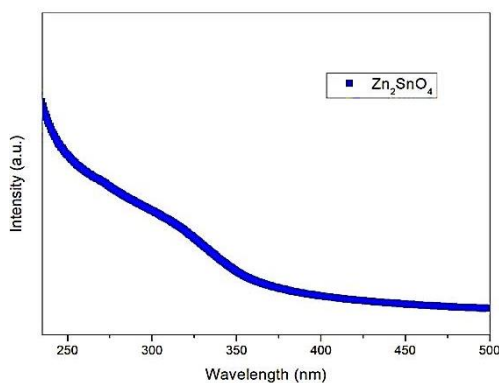


Fig. 2a. The optical absorption spectrum of the catalyst prepared via hydrothermal synthesis method.

It was observed an increase in the absorbance at 305 nm. The determination of the band gap energy of catalyst is obtained by Tauc's relation is given in Equation (2).

$$\alpha h\nu = C(h\nu - E_g)^n \quad (2)$$

where α is the absorption coefficient, $n=1/2$ or 2 for direct or indirect allowed transition, respectively, C is the characteristic parameter for respective transitions, $h\nu$ is photon energy and E_g is energy band gap. The plot of $(\alpha h\nu)^2$ versus $h\nu$ for catalyst is revealed in Fig. 2b.

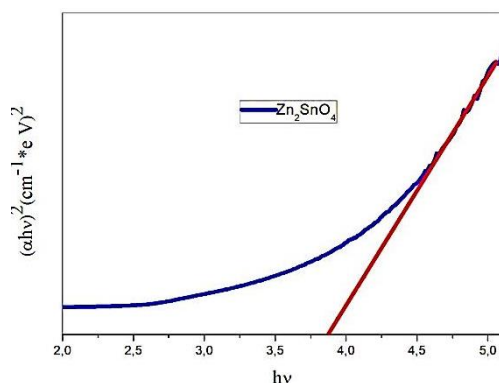


Fig. 2b. The optical absorption spectrum of catalyst prepared via hydrothermal synthesis method.

The band gap of the catalyst was determined as 3.87 eV when the Tauc's region is extrapolated to $(\alpha h\nu)^2 = 0$. It can be clearly seen that the determined band gap energy (3.84 eV) of catalyst is higher than that of bulk ZTO (3.6 eV). The reason of the increment in the band gap energy could be owing to the quantum confinement effect which arises from small particle size.

Photoluminescence measurement

Another tool to study optical properties of semiconductor materials is photoluminescence (PL) spectroscopy. Fig. 3 demonstrates the emission spectrum for catalyst synthesized via hydrothermal synthesis technique.

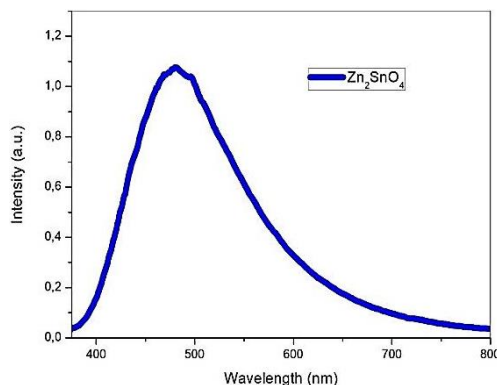


Fig. 3. The emission spectrum for catalyst prepared via hydrothermal synthesis method.

The spectrum was recorded under UV light of 310 nm wavelength as the excitation source. It was observed a PL band at 480 nm which is in the blue region. Yakami et al.[20] reported that the blue emission is usually associated with to radiative recombination of a photo-generated hole

with an electron occupying the oxygen vacancy. Moreover, they mentioned that surface state can be a possible reason for the broad emission on the blue region. It is well known that the lower recombination of excited electrons and electron vacancies result in the lower PL intensity. Thus, it can be said that the observed high PL intensity is shown in Fig. 3 indicates high recombination of electrons and electron vacancies under light irradiation.

Photocatalytic Activity of ZTO Nanoparticles

In order to investigate the effect of the dye concentration on the photocatalytic activity of the catalyst, the amount of dye concentration was varied from 5 to 30 ppm. During this measurement, the amount of the catalyst was kept as 30 mg. Fig. 4 indicates the plot of degradation (%) value, as a function of time, obtained in the presence of the catalyst at different dye concentrations.

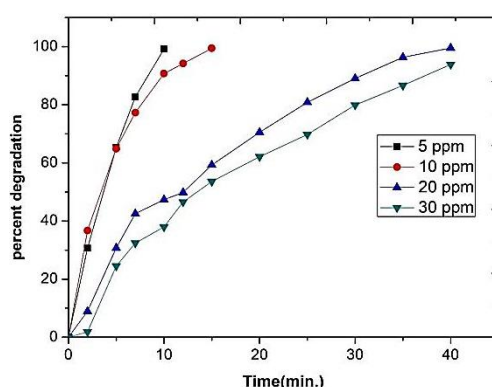


Fig. 4. Degradation (%) value of different dye concentrations (reaction condition: amount of catalyst: 30 mg).

It was observed that the degradation (%) value decreases with the increase in the concentration of methylene blue. The probable cause of this situation can be explained as the increased concentration of dye increases the adsorption capacity on the catalyst surface. This situation reduces the photocatalytic activation by inhibiting the formation of OH^- adsorption on the catalyst surface. Thus, the reduction in the formation of OH^- leads to a reduction in color removal efficiency. Another reason for this is that the increase in initial dye concentration reduces the number of photons. This results in less photon adsorption on the catalyst surface. Another reason for this is that the increase in initial dye concentration reduces the number of photons. This results in less photon adsorption on the catalyst surface and decreases in the reaction time. Mohavedi et al. [21] studied the photocatalytic activity of ZTO nanoparticles (catalyst). They stated that the degradation reaction was completed in 180 minutes in the presence of dye at a concentration of 5 ppm. In contrast to this result, we observed that the reaction was completed in a shorter time (15 minutes) under the same conditions in our study.

One of the most important parameters in photocatalytic studies is the amount of catalyst. In order to investigate the effect of catalyst amount on the photocatalytic activity, the amount of catalyst was varied from 5 to 40 mg. During this measurement, the dye concentration was kept as 10 ppm. Fig. 5 indicates the plot of degradation (%) value, as a function of time, obtained in the presence of different catalyst amount at 10 ppm of dye concentration.

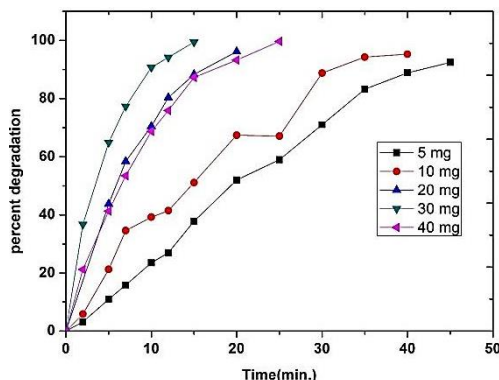


Fig. 5. Degradation (%) value of different amount of catalyst (reaction condition: dye concentration: 5 ppm).

It was observed that when the amount of catalyst is increased from 5 mg to 30 mg, the degradation reaction rate increases. However, when the amount of catalyst is increased to 40 mg, a noticeable decrease in the reaction rate is observed. The possible cause of the increase of the degradation reaction as the amount of catalyst increases is the increase in the adsorption of light and the formation of OH radicals on the catalyst surface due to the increase in the active areas with increasing catalyst amount. In addition, catalyst aggregation may occur if the amount of catalyst is too high. Thus, the rate of degradation reaction is thought to increase as the solid-liquid contact surface will decrease. Similar observation expressed by Xiao et al. [22]. They stated that the excess amount of catalyst blurs the solution and this situation prevents the light to reach the surface of the catalyst.

The reproducibility of the photocatalytic activity of the synthesized catalyst was investigated. The data obtained is shown in Fig. 6.

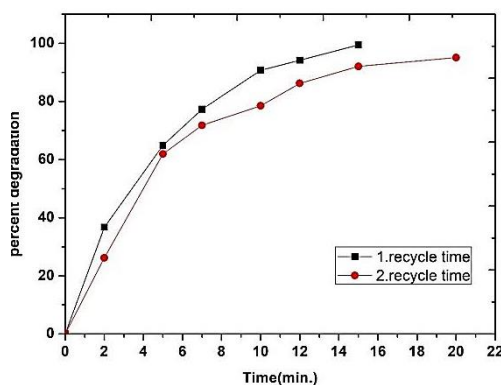


Fig. 6. Re-usability test for synthesized catalyst.

Although the use of the synthesized catalyst for the second time reduces the photocatalytic degradation reaction rate, it is clear that the photocatalytic activity of the catalyst is still effective. The result of the experiment shows that the catalyst can be used for the second time in degradation of the dye.

Photocatalytic degradation kinetics of dye in the presence of catalyst was investigated using first and second-order kinetic models. First and second-order kinetic model relations are given in Equation (3) and Equation (4), respectively.

$$-\ln\left(\frac{C_t}{C_o}\right) = k_1 \cdot t \quad (3)$$

$$\frac{1}{C_t} - \frac{1}{C_o} = k_2 \cdot t \quad (4)$$

where, C_t : solution concentration at time t (mg/l), C_0 : Initial solution concentration (mg/l), k_1 : First order adsorption rate constant (min^{-1}), k_2 : Second order adsorption rate constant ($\text{l} \cdot \text{mg}^{-1} \cdot \text{min}^{-1}$), t : Adsorption time (min.). The graphs obtained from the above equations are given in Fig. 7 (a-b).

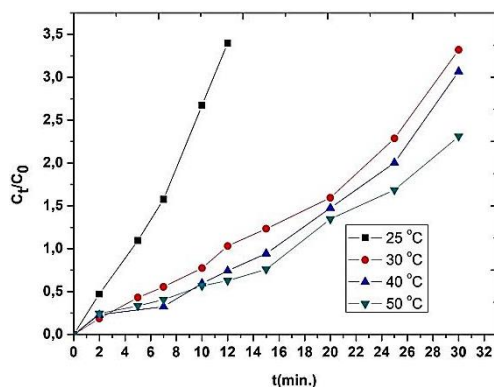


Fig. 7a. The first-order kinetics for photocatalytic degradation of dye in the presence of catalyst.

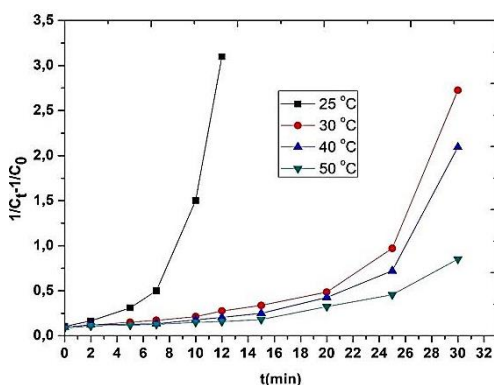


Fig. 7b. The second-order kinetics for photocatalytic degradation of dye in the presence of catalyst.

The constants of the first and second order kinetic models determined by the equations in the graphs given in Figure 7 (a-b) are given in Table 1.

Table 1. First and second order kinetic model constants.

Temperature ($^{\circ}\text{C}$)	First-order kinetic model		Second-order kinetic model	
	k_1 (min.)	R^2	k_1 (min.)	R^2
25	0,2638	0,9786	0,1673	0,6913
40	0,0945	0,9563	0,047	0,5763
50	0,0831	0,9162	0,0355	0,5578
60	0,068	0,9568	0,0164	0,7274

According to the obtained regression coefficient (R^2), photocatalytic degradation kinetics of dye at all temperatures were better matched to the first order kinetic model. Also, it is seen that k_1 value decreases as the temperature increases in both models. This results in a decrease in the

degradation reaction rate of dye as the temperature increases. The probable cause of this situation can be explained by the effect of ambient temperature on the efficiency of semiconductor-based catalysts.

4. Conclusions

Nanosized ZTO nanoparticles were synthesized via the hydrothermal technique. It was observed that ZTO nanoparticles have the formation of face-centered cubic spinel structure with the lattice constant $a = 8.66 \text{ \AA}$. The average crystallite size of the nanoparticles was calculated as 18.75 nm by using the Debye–Scherrer equation. The band gap of ZTO nanoparticles was determined as 3.87 eV when the Tauc's region is extrapolated to $(\alpha h\nu)^2 = 0$. It can be clearly seen that the determined band gap energy (3.84 eV) of the catalyst is higher than that of bulk ZTO (3.6 eV). It was detected a PL band for ZTO nanoparticles at 480 nm which is in the blue region. The effect of some parameters (amount of dye, amount of catalyst and temperature) were studied on the photocatalytic activity of ZTO nanoparticles. The obtained all results revealed that ZTO nanoparticles can be used as promising photocatalysts for degradation methyl-blue (MB) (dye). Moreover, it was determined that photocatalytic degradation kinetics of dye at all temperatures are better matched to the first order kinetic model.

References

- [1] O. Ola, M. M. Maroto-Valer, *Journal of Photochemistry and Photobiology C: Photochemistry Reviews* **24**, 16 (2015).
- [2] G. Song et al., *Frontiers of Chemical Science and Engineering* **11**(2), 197 (2017).
- [3] M. Watanabe, *Science and technology of advanced materials* **18**(1), 705 (2017).
- [4] V. Binas et al., *Journal of Materiomics* **3**(1), 3 (2017).
- [5] S. Dinesh, et al., *Journal of Materials Science: Materials in Electronics* **27**(9), 9668 (2016).
- [6] S. Anandan, Y. Ikuma, K. Niwa, *Solid State Phenomena* **162**, 239 (2010).
- [7] A. Phaniendra, D. B. Jestadi, L. Periyasamy, *Indian journal of clinical biochemistry: IJCB*, **30**(1), 11 (2015).
- [8] R. Saravanan, F. Gracia, A. Stephen, *Nanocomposites for Visible Light-induced Photocatalysis*, M.M. Khan, D. Pradhan, and Y. Sohn, Editors. 2017, Springer International Publishing: Cham. p. 19-40.
- [9] V. L. P. V. Rajagopalan, *Scientific Reports* **6**, 38606 (2016).
- [10] A. Annamalai et al., *Materials Characterization* **62**(10), 1007 (2011).
- [11] S. Sharma, M. Kumar, S. Chhoker, *Vacuum*, 2018.
- [12] S. Sun, S. Liang, *Journal of Materials Chemistry A* **5**(39), 20534 (2017).
- [13] U. Hameed, K. Asma, A. Zareen, *Materials Research Express*. **1**(4), 045001 (2014).
- [14] D. An et al., *Sensors and Actuators B: Chemical* **213**, 155 (2015).
- [15] W. Tang et al., *Journal of Materials Science* **49**(3), 1246 (2014).
- [16] W. Cun et al., *Journal of Materials Science* **37**(14), 2989 (2002).
- [17] K. Byrappa, T. Adschiri, *Progress in Crystal Growth and Characterization of Materials* **53**(2), 117 (2007).
- [18] V. Šepelák et al., *Journal of Materials Chemistry* **22**(7), 3117 (2012).
- [19] L. Allwin Joseph et al., *Nanoparticles* **2016**, 1-6 (2016).
- [20] B. R. Yakami et al., *Journal of Applied Physics* **120**(16), 163101 (2016).
- [21] M. Movahedi et al., *Applied Chemistry* **11**(41), 11 (2016).
- [22] Q. Xiao, et al., *Solar Energy* **82**(8), 706 (2008).